Spin-Polarization Control Driven by a Rashba-Type Effect Breaking the Mirror Symmetry in Two-Dimensional Dual Topological Insulators

Carlos Mera Acosta[*] and Adalberto Fazzio

*Institute of Physics, University of Sao Paulo, CP 66318, 05315-970 Sao Paulo, SP, Brazil
and Brazilian Nanotechnology National Laboratory, CP 6192, 13083-970 Campinas, SP, Brazil*

Three-dimensional topological insulators protected by both the time reversal (TR) and mirror symmetries were recently predicted and observed. Two-dimensional materials featuring this property and their potential for device applications have been less explored. We find that, in these systems, the spin polarization of edge states can be controlled with an external electric field breaking the mirror symmetry. This symmetry requires that the spin polarization is perpendicular to the mirror plane; therefore, the electric field induces spin-polarization components parallel to the mirror plane. Since this field preserves the TR topological protection, we propose a transistor model using the spin direction of protected edge states as a switch. In order to illustrate the generality of the proposed phenomena, we consider compounds protected by mirror planes parallel and perpendicular to the structure, e.g., Na_3Bi and half-functionalized (HF) hexagonal compounds, respectively. For this purpose, we first construct a tight-binding effective model for the Na_3Bi compound and predict that HF-honeycomb lattice materials are also dual topological insulators.

The quantum geometrical description of the insulator state gave rise to a breakthrough in the understanding of the topological phases in solids [1–4]. Topological invariants, e.g., the Z_2 invariant and the Chern number $\mathcal{C}_n$, classify insulators according to the preserved symmetries and the "symmetry-charge" pumped to the boundary [5]. Systems featuring a nonzero topological invariant, i.e., topological insulators (TIs), support dissipationless metallic boundary (edge or surface) states protected by a specific crystal symmetry on a bulk insulator [6]. For instance, quantum spin Hall insulators (QSHIs) and topological crystalline insulators (TCIs) are two-dimensional (2D) materials characterized by $Z_2 = 1$ [7–9] and a nonzero mirror Chern number [10–12], $\mathcal{C}_M$, respectively. In QSHIs, the edge states are protected by the time-reversal (TR) symmetry, while in TCIs by either point or mirror symmetries. Topological transitions are typically related to band inversions [13]: the transition from normal insulators to either QSHIs or TCIs with $\mathcal{C}_M = \pm 1$ requires an odd number of band inversions, while TCIs with $\mathcal{C}_M = \pm 2$ exhibit even band inversions. Naturally, $\mathcal{C}_M \neq 0$ or ± 2 intrinsically avoid the QSH state ($Z_2 = 1$).

Materials with a dual topological character (DTC), i.e., systems that are simultaneously QSHIs (TIs in three dimensions) and TCIs [14], requires both $Z_2 = 1$ and $\mathcal{C}_M = \pm 1$, which imposes a condition: it must occur only an odd number of band inversion at k points, preserving both the mirror and the TR symmetries. In view of the TR invariant momentum points always come in pairs, this condition is only satisfied by the Γ point. Since 2D-TCIs are typically systems with $\mathcal{C}_M = \pm 2$, e.g., SnTe multilayers [11,15], monolayers of SnSe, PbTe, PbSe [16–18], TlSe [19], and SnTe/NaCl quantum wells [20], DTC in 2D compounds have been predicted only for Na_3Bi layers [21]. Three-dimensional materials exhibiting DTC not only have been predicted in Bi_2Te_3 [14], Bi_4Se_3 [22], and $Bi_{1-x}Sb_x$ [23], but also experimentally observed in the stoichiometric superlattice $[Bi_2]_1[Bi_2Te_3]_2$ [24].

The search for novel systems featuring DTC and the study of their potential for device applications is desired for the development of spintronics. For instance, in systems featuring DTC, external electric and magnetic fields allow the control of topological states. This intrinsic property arises from the possible separate manipulation of QSHI [25–27] and TCI [28–30] states due to the symmetry breaking induced by the external fields; i.e., the magnetic (electric) field breaks the TR (mirror) symmetry, but the edge states could still be protected by the mirror (TR) symmetry.

In this Letter, we propose the control of the edge states spin-polarization orientation through an external electric field breaking the mirror symmetry in systems exhibiting DTC; i.e., this field induced a Rashba-type effect resulting in spin-polarization components parallel to the mirror plane. Based on this effect, we suggest a transistor model using the spin direction as a switch. In order to illustrate the generality of the proposed phenomena, we consider compounds protected by mirror planes parallel and perpendicular to the structure, e.g., Na_3Bi and half-functionalized (HF) hexagonal compounds, respectively. For this purpose, we first (i) construct a tight-binding effective model for the Na_3Bi compound [21], and

(ii) predict that the TR-symmetry protected edges states in HF-honeycomb lattice materials (Ref. [31]) are also protected by mirror planes perpendicular to the layer, which is different from the conventional TCIs. Using the proposed models, we then study the in- and out-plane electric field breaking the mirror symmetry in Na_3Bi and HF-hexagonal compounds, verifying the change of the spin polarization in TR-symmetry protected edge states.

Effective Hamiltonian describing the DTC of Na_3Bi.— The Na_3Bi compound satisfies the symmetry operations: (i) threefold rotation symmetry $\mathcal{R}_3$ along the z axis, (ii) TR symmetry $\mathcal{T}$, (iii) mirror symmetry $\mathcal{M}_x$ ($x \to -x$), and (iv) mirror symmetry $\mathcal{M}_z$ ($z \to -z$). The TC phase is protected by the reflection symmetry respect to the plane containing the 2D layer, i.e., M_z, which is schematically represented in Fig. 1. In the inverted order, the valence band maximum (VBM) has a p-orbital character, mainly dominated by p_z and s orbitals of the Bi atoms, whereas the conduction band minimum (CBM) mainly consists of $p_{x,y}$-Bi orbitals. At the Γ point, the valence (conduction) band is described by the effective states $\{|Bi_J, j_z\rangle\}$ with the total angular momentum $J = 3/2$ ($J = 1/2$), i.e, $|Bi_{1/2}, \pm 1/2\rangle$ and $|Bi_{3/2}, \pm 1/2\rangle$, respectively. Using the symmetry operations for these states, we find an effective tight-binding Hamiltonian model describing the Na_3Bi band structure near the Fermi energy (see Supplemental Material [32]). In the limit $\vec{k} \to \Gamma$, the effective Hamiltonian reads

(a)

● Bi
● ● Na

● V
● IV
● VII

(b)
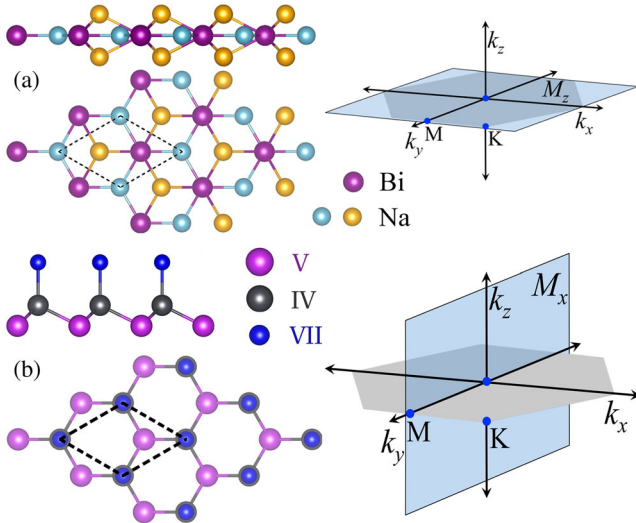
FIG. 1. Side and top view of the (a) Na_3Bi and (b) HF honeycomb lattice compounds. Unit cells are represented by the dashed lines and the respective Brillouin Zone (BZ) in gray. The mirror planes given rise to the TCI state are represented by the blue planes. For HF compounds, there are three equivalent reflection planes containing the line connecting two TR invariant equivalent M points. For illustrative purpose, we only show the plane giving the reflection $x \to -x$.

$$\mathcal{H}_{Na_3Bi} = \begin{pmatrix} -\varepsilon + \xi k^2 & 0 & 0 & \ell_-(\vec{k}) \\ 0 & -\varepsilon + \xi k^2 & \ell_+(\vec{k}) & 0 \\ 0 & \ell_-(\vec{k}) & \tilde{\varepsilon} - \tilde{\xi}k^2 & 0 \\ \ell_+(\vec{k}) & 0 & 0 & \tilde{\varepsilon} - \tilde{\xi}k^2 \end{pmatrix},$$

(1)

where $k_\pm = k_x \pm ik_y$ and $k_2 = k_x^2 + k_y^2$. Here, $\ell\pm = \gamma k_\pm + \tilde{\gamma}k_\mp^2$ is the interaction term between the $J = 1/2$ and $J = 3/2$ states. The on-site energy (mass term) and the kinetic term for states with $J = 1/2$ ($J = 3/2$) are represented by ε and ξ ($\tilde{\varepsilon}$ and $\tilde{\xi}$), respectively. This model reproduces our density functional theory (DFT) calculation, performed using the SIESTA code [33] with the on-site approximation for the SOC [34,35] and the Perdew-Burke-Ernzenhof generalized gradient approximation [36] for the exchange-correlation functional.

The mirror symmetry protection becomes evident when the Hamiltonian is written in the basis formed by the mirror operator eigenvectors. For any generic $\vec{k}$ point in the BZ, the wave function $|\psi_n^\sigma(k_x, k_y)\rangle$ (with $\sigma = \uparrow, \downarrow$) can be indexed with the eigenvalues of the mirror operator $\mathcal{M}_z$, $m_{z,J}$. This is a consequence of commutation relation $[\mathcal{H}(k_x, k_y), \mathcal{M}_z]$, which can be easily verified using the matrix representation $\mathcal{M}_z = -i\tau_z \otimes \sigma_z$; i.e., the mirror operator $\mathcal{M}_z$ transforms the orbitals as $\mathcal{M}_z|Bi_{1/2}, \pm 1/2\rangle = \mp i|Bi_{1/2}, \pm 1/2\rangle$ and $\mathcal{M}_z|Bi_{3/2}, \pm 1/2\rangle = \pm i|Bi_{3/2}, \pm 1/2\rangle$. Using this representation, we find the eigenvalues $m_{z,1/2} = \pm i$ and $m_{z,3/2} = \pm i$, and the eigenvectors $\phi_{z,1/2}^{\pm i} = (\mathcal{Z}_{\pm i}\vec{0})$ and $\phi_{z,3/2}^{\pm i} = (\vec{0}\mathcal{Z}_{\mp i})$. Here, $\vec{\mathcal{Z}}_i = (1\ 0)$, $\mathcal{Z}_{-i} = (0\ 1)$, and $\vec{0} = (0\ 0)$. The Hamiltonian in the basis $\{\phi_{z,1/2}^i, \phi_{z,3/2}^i, \phi_{z,1/2}^{-i}, \phi_{z,3/2}^{-i}\}$ is a block diagonal matrix,

$$\mathcal{H}_{Na_3Bi} = \begin{pmatrix} h_{z,i}(\vec{k}) & 0 \\ 0 & h_{z,-i}(\vec{k}) \end{pmatrix},$$

(2)

where the blocks describing the mirror projected states read

$$h_{z,\pm i}(k_x, k_y) = \begin{pmatrix} -\varepsilon + \xi k^2 & \ell_\pm(\vec{k}) \\ \ell_\mp(\vec{k}) & \tilde{\varepsilon} - \tilde{\xi}k^2 \end{pmatrix}.$$

(3)

Thus, a perturbation breaking the mirror symmetry introduces off-diagonal matrix elements in Eq. (2). For instance, according to our *ab initio* calculations, a perpendicular electric field can be effectively included as a Rashba-type term that couples the Hamiltonians $h_{z,i}$ and $h_{z,-i}$, i.e., $h_R = i\lambda_R k_-$ (see Supplemental Material [32]).

The mirror Chern number, $\mathcal{C}_M$, is defined in terms of the states at the mirror symmetry invariant k points. For instance, in the 3D-TCI SnTe, $\mathcal{C}_M$ is computed using only the k points at the intersection between the mirror plane and

the 3D BZ. Here, since the intersection between the BZ and the mirror plane is the BZ itself, all k points are mirror symmetry invariant. Thus, $\mathcal{C}_M$ is calculated through the Berry phase, $\Omega_n^{\pm i}(k_x, k_y)$, defined in the whole BZ [10,19], i.e., $\mathcal{C}_M = (\mathcal{C}_i - \mathcal{C}_{-i})/2$, where $\mathcal{C}_{\pm i}$ is the Chern number for mirror eigenvalues $\pm i$,

$$\mathcal{C}_{\pm i} = \frac{1}{2\pi} \sum_{n<E_f} \int_{\text{BZ}} \Omega_n^{\pm i}(k_x, k_y) dx dy. \qquad (4)$$

Using the proposed model, we verified that $\mathcal{C}_{\pm i} = \mp 1$, indicating that the Na$_3$Bi monolayer is a TCI with $\mathcal{C}_M = -1$, as predicted in Ref. [21].

Prediction of DTC in HF-honeycomb materials.—Graphene-like materials functionalized with group-VII atoms are predicted to behave as QSHIs [37]. When a VII atom is removed from the unit cell, one sublattice exhibits dangling bonds, and, hence, magnetic moments due to unpaired electrons possibly spontaneously evolve into a magnetic order, spoiling the QSH states and given rise to the quantum anomalous Hall effect [38]. The electrons can be paired by substituting the nonpassivated IV atoms by atoms with an odd number of valence electrons. Thus, HF IV–V hexagonal-lattices materials, formed by two triangular sublattices, one consisting of an IV–VII dimer and the other of atoms V (see Fig. 1), have no magnetic moment. Therefore, this systems are predicted to be mechanically stable QSHIs [31]. Since the functionalization breaks the mirror symmetry $\mathcal{M}_z$, the symmetry operation satisfied by HF compounds are only $\mathcal{R}_3$, $\mathcal{T}$, and $\mathcal{M}_x$, which is schematically represented in Fig. 1(b). In these systems, the TCI phase is protected by the reflection symmetry in respect to the three planes that are perpendicular to the lattice and contain the lines connecting the nearest neighbors in the honeycomb lattice.

HF-honeycomb lattice materials can display an inverted band character dominated by Bi-atomic orbitals, like the Na$_3$Bi compound. Similarly, in the inverted order, the VBM has a p-orbital character, mainly dominated by p_z-Bi orbitals, whereas the CBM at Γ mainly consists of $p_{x,y}$-Bi orbitals. Hence, the Hamiltonian in the full SOC basis $\{|\text{Bi}_{1/2}, \pm 1/2\rangle, |\text{Bi}_{3/2}, \pm 1/2\rangle\}$ reads [31]

$$\mathcal{H}_{\text{HF}} = \begin{pmatrix} -\varepsilon + \xi k^2 & i\alpha k_- & 0 & \gamma k_- \\ -i\alpha k_+ & -\varepsilon + \xi k^2 & \gamma k_+ & 0 \\ 0 & \gamma k_- & \tilde{\varepsilon} - \tilde{\xi} k^2 & 0 \\ \gamma k_+ & 0 & 0 & \tilde{\varepsilon} - \tilde{\xi} k^2 \end{pmatrix}, \quad (5)$$

where α_R is the Rhasba parameter, and γ is the interaction term between the $J = 1/2$ and $J = 3/2$ states.

The Hamiltonian describing QSHIs with inversion symmetry breaking [Eq. (5)] leads to parabolic bands with the same helical in-plane spin texture, forbidding the

backscattering in bulk states [31]. This unconventional spin topology was also observed in the nontopological alloy Bi/Cu(111) [39]. We find that the scattering processes are not only limited by the spin texture. Specifically, since the commutation relation $[\mathcal{H}(k_x = 0), \mathcal{M}_x]$, the wave function can be indexed with the eigenvalues of the mirror operator $\mathcal{M}_x$, $m_{x,J}$, for $k_x = 0$. In the basis $\{\phi_{x,1/2}^i, \phi_{x,3/2}^i, \phi_{x,1/2}^{-i}, \phi_{x,3/2}^{-i}\}$, the Hamiltonian is a block diagonal matrix,

$$\tilde{\mathcal{H}}(\vec{k})|_{k_x=0} = \mathbb{1} \otimes h_0 + \tau_z \otimes (h - h_R), \qquad (6)$$

where $h = \sigma_y \gamma k$ and $h_R = (\mathbb{1} + \sigma_z)\alpha k/2$, and

$$h_0(k) = \begin{pmatrix} -\varepsilon + \xi k^2 & 0 \\ 0 & \tilde{\varepsilon} - \tilde{\xi} k^2 \end{pmatrix}. \qquad (7)$$

The blocks of the Hamiltonian related to the eigenvalues of the mirror symmetry operator $\pm i$ are written as $h_{\pm i} = h_0 \pm (h - h_R)$, respectively. The Hamiltonian $h_{\pm i}$ leads to the band structure discriminating mirror eigenvalues. Since the intersection between the mirror plane and the BZ is a line (see Fig. 1), the mirror Chern number is defined in terms of the one-dimensional k points at $k_x = 0$. Specifically, $\mathcal{C}_{\pm i}$ are calculated via the winding numbers [40], which is essentially the Zak phase for the one-dimensional effective Hamiltonian $h_{\pm i}$ [41–43]. Remarkably, in the HF-honeycomb material, the edge states are protected by the mirror plane perpendicular to the structure ($\mathcal{M}_x$), which is different from the conventional TCIs. This offers the possibility of breaking both TR and mirror symmetries with a perpendicular magnetic field (parallel to the mirror plane $\mathcal{M}_x$) and also allows us to manipulate the edge states with in-plane magnetic fields (see Supplemental Material [32]). In the general case, the magnetic field $\mathcal{H}_{B_{\parallel \mathcal{M}_x}} = \mathbb{1} \otimes (\sigma_y B_y + \sigma_z B_z)$, gives rise to a coupling term between h_i and h_{-i}, inducing a spin polarization in the direction in which it is applied, even for the k point at the mirror plane.

Electric field effect in 2D materials with DTC.—Metallic edge states, the most interesting feature in both TCIs and QSHIs, are computed by considering open boundary conditions in the previously discussed tight-binding models. First, we confirm the presence of edge states preserving the TR symmetry, i.e., antipropagating spin current in each edge. Before including the electric field effects, the spin is forced to be perpendicular to the mirror plane to preserve this symmetry, i.e., oriented along the z axis (x axis) in Na$_3$Bi (HF-hexagonal) compounds, as shown in Figs. 2 and 3. This suggests that external perturbations breaking the mirror symmetry could induce spin-polarization components parallel to the mirror plane, as we show below by considering an external electric field.
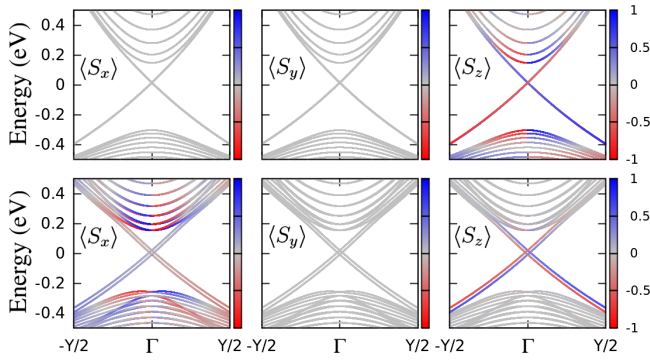
FIG. 2. Expected values of the spin operator for the band structure of a Na_3Bi nanoribbon 37.1 nm width armchair terminated for (top) $E_0 = 0$ V/Å and (bottom) $E_0 = 0.1$ V/Å. Here, E_0 is an external electric field breaking the mirror symmetry $\mathcal{M}_z$. The color code stands for the spin orientation.

In the Na_3Bi compound, a perpendicular electric field breaks the symmetry M_z, as previously discussed. This field induces a helical spin texture in the bulk band structure, leading to in-plane spin-polarization components in the edge states, i.e., parallel to M_z, as represented in Fig. 2. The edge states are still protected by the TR symmetry and the electric field provides a mechanism to change the spin-polarization orientation.

An external electric field breaking the mirror symmetry $\mathcal{M}_x$ can be introduced by modifying the on-site term, i.e., $\tilde{\varepsilon}_n(\vec{k}) = \varepsilon(\vec{k}) + nae E_0/N$, where n is the index of the Bi atoms in a nanoribbon formed by N unit cells along the x axis, a is the lattice constant, and e is the electron charge. We find that this field induces a nonzero, out-plane spin-polarization, as represented in Fig. 3.

The effect of an electric field breaking the mirror symmetry can be understood using the phenomenological model describing the Rashba effect in inversion symmetry breaking systems: the electric field $\vec{E}$ induces a momentum-dependent Zeeman energy $\vec{\phi}_{\rm eff} = \mu_B \vec{\mathcal{B}}_{\rm eff} \sigma$ with $\vec{\mathcal{B}}_{\rm eff} = \vec{E} \times \hbar \vec{k}/m_e c^2$ [44,45]. This odd-in-k effective field, i.e., $\vec{\mathcal{B}}_{\rm eff}(k) = -\vec{\mathcal{B}}_{\rm eff}(-k)$, preserves the TR symmetry and only appears when the mirror symmetry is broken, in the same way that the Rashba effect depends on the inversion symmetry breaking [45,46]. Analogous to the generic helical edge states [47,48], this field changes the direction of the spin polarization, as observed in Figs. 2 and 3. Specifically, in armchair nanoribbons, the momentum carried by the electrons at the edge is oriented along the y axis. In HF-honeycomb (Na_3Bi) compounds, the external electric field is transverse (perpendicular) to the nanoribbon $\vec{E} = E_0 \hat{x}$ ($\vec{E} = E_0 \hat{z}$), resulting in an effective field along the z axis (x axis), $\mathcal{B}_{\rm eff} = (\mu_B/m_e c^2) E_0 k_y$.

The mirror symmetry protection in HF-hexagonal materials implies that states spatially localized in different edges have the same momentum and spin direction. Thus, the spin
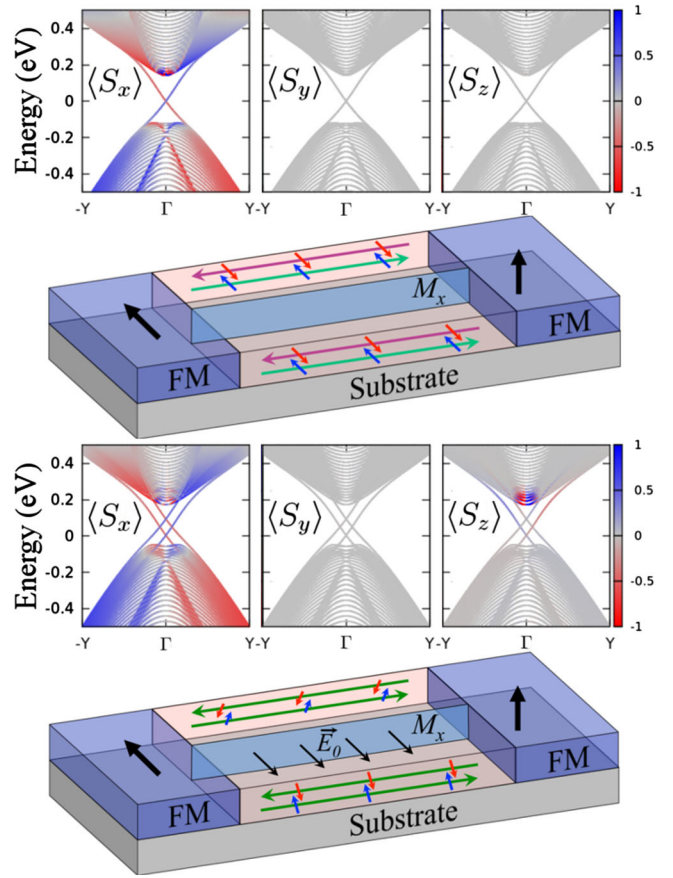
FIG. 3. Expected values of the spin operator for the band structure of a nanoribbon 33.6 nm width armchair terminated for (top) $E_0 = 0$ V/Å and (bottom) $E_0 = 2.67 \times 10^{-2}$ V/Å. Here, E_0 is an external electric field breaking the mirror symmetry $\mathcal{M}_x$ (blue plane). The color code stands for the spin orientation. The spin texture is also schematically represented in a transistor model: a nanoribbon connected to two ferromagnetic contacts (FM). This structure is deposited in a substrate (gray area). States with eigenvalue symmetry operator $\pm i$, which are only defined if the electric field is zero, are represented by purple and green, respectively.

flip is required in scattering processes involving these states. This spin texture has also been observed in curved QSHIs [49]. In zigzag nanoribbons, the mirror symmetry is intrinsically broken and, hence, the spin is not only oriented along the x axis [31]. Although giant Rashba splitting coexists with surface states in the 3D TIs due to the band bending and structural inversion asymmetry [50–52], the consequences of the Rashba effect and transverse electric fields in surface states have not been widely explored [53]. Based on the tight-binding model proposed in Ref. [54], we verify that spin polarization can also be controlled in 3D TIs with DTC (see Supplemental Material [32]). The spin-polarization control proposed in this Letter is different from the dynamic spin-orbit torque in anti- and ferromagnetic 2D and 3D TIs [55–59], since the effective field $\vec{\mathcal{B}}_{\rm eff}$ appears

for the equilibrium carrier spin density configuration and does not require magnetic order.

The change of spin orientation suggests that a simple transistor model can be constructed. If the armchair nanoribbon of HF-honeycomb materials (Na_3Bi) is connected to ferromagnetic electrodes, the electrons in the edge states are not detected by a drain whose magnetic moment is perpendicular to the x axis (z axis), as schematically represented in Fig. 3. This corresponds to the off of the transistor. If an electric field perpendicular to the mirror plane is turned on, the electrons in the edge states have a nonzero probability of being detected by the electrode (see Fig. 3). Different from the transistors based on TCIs, in DTC insulators, the switch is not defined by the band gap opening, but the spin-polarization direction.

Summarizing, we proposed a transistor model using the spin direction as a switch. We showed that in systems simultaneously protected by the TR and mirror symmetries, the spin polarization is always perpendicular to the mirror plane protecting the metallic edge states. We demonstrated that an external electric field breaking the mirror symmetry induces a spin polarization parallel to the mirror plane. Since the electric field does not break the TR symmetry, the metallic edge states are still protected by this symmetry, which allows the control of the spin polarization, preserving the Dirac cone formed by these states. We constructed tight-binding models for Na_3Bi and HF-honeycomb materials. Using this model we computed the mirror Chern number, predicting the DTC in HF-honeycomb materials and verifying this behavior in the Na_3Bi compound, which are protected by the mirror plane $\mathcal{M}_x$ and $\mathcal{M}_z$, respectively. In order to illustrate that the proposed spin-polarization control does not depend on the mirror plane orientation, we study this effect in both materials, the only two-dimensional systems predicted to exhibit a DTC. In light of recent advances in the application of electric fields in the 2D Na_3Bi [60], the practical realization of the proposed device is feasible.

---

*acosta@if.usp.br

[1] D. J. Thouless, M. Kohmoto, M. P. Nightingale, and M. den Nijs, Phys. Rev. Lett. **49**, 405 (1982).

[2] R. Resta, Eur. Phys. J. B **79**, 121 (2011).

[3] R. Resta, Europhys. Lett. **22**, 133 (1993).

[4] M. Z. Hasan and C. L. Kane, Rev. Mod. Phys. **82**, 3045 (2010).

[5] L. Fu and C. L. Kane, Phys. Rev. B **74**, 195312 (2006).

[6] X.-L. Qi and S.-C. Zhang, Rev. Mod. Phys. **83**, 1057 (2011).

[7] C. L. Kane and E. J. Mele, Phys. Rev. Lett. **95**, 226801 (2005).

[8] C. L. Kane and E. J. Mele, Phys. Rev. Lett. **95**, 146802 (2005).

[9] L. Fu and C. L. Kane, Phys. Rev. B **76**, 045302 (2007).

[10] L. Fu, Phys. Rev. Lett. **106**, 106802 (2011).

[11] T. H. Hsieh, H. Lin, J. Liu, W. Duan, A. Bansil, and L. Fu, Nat. Commun. **3**, 982 (2012).

[12] Y. Ando and L. Fu, Annu. Rev. Condens. Matter Phys. **6**, 361 (2015).

[13] A. Bansil, H. Lin, and T. Das, Rev. Mod. Phys. **88**, 021004 (2016).

[14] T. Rauch, M. Flieger, J. Henk, I. Mertig, and A. Ernst, Phys. Rev. Lett. **112**, 016802 (2014).

[15] Y. Tanaka, Z. Ren, T. Sato, K. Nakayama, S. Souma, T. Takahashi, K. Segawa, and Y. Ando, Nat. Phys. **8**, 800 (2012).

[16] E. O. Wrasse and T. M. Schmidt, Nano Lett. **14**, 5717 (2014).

[17] J. Liu, X. Qian, and L. Fu, Nano Lett. **15**, 2657 (2015).

[18] C. Niu, P. M. Buhl, G. Bihlmayer, D. Wortmann, S. Blugel, and Y. Mokrousov, Phys. Rev. B **91**, 201401 (2015).

[19] C. Niu, P. M. Buhl, G. Bihlmayer, D. Wortmann, S. Blgel, and Y. Mokrousov, Nano Lett. **15**, 6071 (2015).

[20] C. Niu, P. M. Buhl, G. Bihlmayer, D. Wortmann, S. Blgel, and Y. Mokrousov, 2D Mater. **3**, 025037 (2016).

[21] C. Niu, P. M. Buhl, G. Bihlmayer, D. Wortmann, Y. Dai, S. Blugel, and Y. Mokrousov, Phys. Rev. B **95**, 075404 (2017).

[22] A. P. Weber, Q. D. Gibson, H. Ji, A. N. Caruso, A. V. Fedorov, R. J. Cava, and T. Valla, Phys. Rev. Lett. **114**, 256401 (2015).

[23] J. C. Y. Teo, L. Fu, and C. L. Kane, Phys. Rev. B **78**, 045426 (2008).

[24] M. Eschbach, M. Lanius, C. Niu, E. Młyńczak, P. Gospodarič, J. Kellner, P. Schüffelgen, M. Gehlmann, S. Döring, E. Neumann, M. Luysberg, G. Mussler, L. Plucinski, M. Morgenstern, D. Grützmacher, G. Bihlmayer, S. Blügel, and C. M. Schneider, Nat. Commun. **8**, 14976 (2017).

[25] X. Qian, J. Liu, L. Fu, and J. Li, Science **346**, 1344 (2014).

[26] K. Olejnik, J. Wunderlich, A. C. Irvine, R. P. Campion, V. P. Amin, J. Sinova, and T. Jungwirth, Phys. Rev. Lett. **109**, 076601 (2012).

[27] D. Nanclares, L. R. F. Lima, C. H. Lewenkopf, and L. G. G. V. Dias da Silva, Phys. Rev. B **96**, 155302 (2017).

[28] J. Liu, T. H. Hsieh, P. Wei, W. Duan, J. Moodera, and L. Fu, Nat. Mater. **13**, 178 (2014).

[29] Y. Okada, M. Serbyn, H. Lin, D. Walkup, W. Zhou, C. Dhital, M. Neupane, S. Xu, Y. J. Wang, R. Sankar, F. Chou, A. Bansil, M. Z. Hasan, S. D. Wilson, L. Fu, and V. Madhavan, Science **341**, 1496 (2013).

[30] P. Dziawa, B. J. Kowalski, K. Dybko, R. Buczko, A. Szczerbakow, M. Szot, E. Łusakowska, T. Balasubramanian, B. M. Wojek, M. H. Berntsen, O. Tjernberg, and T. Story, Nat. Mater. **11**, 1023 (2012).

[31] C. Mera Acosta, O. Babilonia, L. Abdalla, and A. Fazzio, Phys. Rev. B **94**, 041302 (2016).

[32] See Supplemental Material at http://link.aps.org/supplemental/10.1103/PhysRevLett.122.036401 for the construction of the tight binding model for the Na_3Bi compound with and without electric fields; the calculation of the mirror Chern number, magnetic field effects, hybrid functional HSE06 band structure, and edge states for

Half-functionalized honeycomb materials; and the discussion about the spin polarization electrical control in similar materials and three-dimensional compounds with DTC.

[33] J. M. Soler, E. Artacho, J. D. Gale, A. García, J. Junquera, P. Ordejón, and D. Sánchez-Portal, J. Phys. Condens. Matter **14,** 2745 (2002).

[34] C. M. Acosta, M. P. Lima, R. H. Miwa, A. J. R. da Silva, and A. Fazzio, Phys. Rev. B **89,** 155438 (2014).

[35] L. Fernandez-Seivane, M. A. Oliveira, S. Sanvito, and J. Ferrer, J. Phys. Condens. Matter **18,** 7999 (2006).

[36] J. P. Perdew, K. Burke, and M. Ernzerhof, Phys. Rev. Lett. **77,** 3865 (1996).

[37] C. Mera Acosta, R. Ouyang, A. Fazzio, M. Scheffler, L. M. Ghiringhelli, and C. Carbogno, arXiv:1805.10950.

[38] S.-C. Wu, G. Shan, and B. Yan, Phys. Rev. Lett. **113,** 256401 (2014).

[39] H. Mirhosseini, J. Henk, A. Ernst, S. Ostanin, C. T. Chiang, P. Yu, A. Winkelmann, and J. Kirschner, Phys. Rev. B **79,** 245428 (2009).

[40] M. Okamoto, Y. Takane, and K.-I. Imura, Phys. Rev. B **89,** 125425 (2014).

[41] L. Li, C. Yang, and S. Chen, Europhys. Lett. **112,** 10004 (2015).

[42] J. Zak, Phys. Rev. Lett. **62,** 2747 (1989).

[43] M. Atala, M. Aidelsburger, J. T. Barreiro, D. Abanin, T. Kitagawa, E. Demler, and I. Bloch, Nat. Phys. **9,** 795 (2013).

[44] Y. A. Bychkov and E. I. Rashba, JETP Lett. **39,** 78 (1984).

[45] A. Manchon, H. C. Koo, J. Nitta, S. M. Frolov, and R. A. Duine, Nat. Mater. **14,** 871 (2015).

[46] S. Vajna, E. Simon, A. Szilva, K. Palotas, B. Ujfalussy, and L. Szunyogh, Phys. Rev. B **85,** 075404 (2012).

[47] L. Ortiz, R. A. Molina, G. Platero, and A. M. Lunde, Phys. Rev. B **93,** 205431 (2016).

[48] D. G. Rothe, R. W. Reinthaler, C.-X. Liu, L. W. Molenkamp, S.-C. Zhang, and E. M. Hankiewicz, New J. Phys. **12,** 065012 (2010).

[49] B. Huang, K.-H. Jin, B. Cui, F. Zhai, J. Mei, and F. Liu, Nat. Commun. **8,** 15850 (2017).

[50] M. Bianchi, D. Guan, S. Bao, J. Mi, B. B. Iversen, P. D. C. King, and P. Hofmann, Nat. Commun. **1,** 128 (2010).

[51] P. D. C. King et al., Phys. Rev. Lett. **107,** 096802 (2011).

[52] H. M. Benia, A. Yaresko, A. P. Schnyder, J. Henk, C. T. Lin, K. Kern, and C. R. Ast, Phys. Rev. B **88,** 081103 (2013).

[53] G. Liu, G. Zhou, and Y.-H. Chen, Appl. Phys. Lett. **99,** 222111 (2011).

[54] C. M. Acosta, M. P. Lima, A. J. R. da Silva, A. Fazzio, and C. H. Lewenkopf, Phys. Rev. B **98,** 035106 (2018).

[55] I. Mihai Miron, G. Gaudin, S. Auffret, B. Rodmacq, A. Schuhl, S. Pizzini, J. Vogel, and P. Gambardella, Nat. Mater. **9,** 230 (2010).

[56] S. Ghosh and A. Manchon, Phys. Rev. B **95,** 035422 (2017).

[57] Y. Wang, P. Deorani, K. Banerjee, N. Koirala, M. Brahlek, S. Oh, and H. Yang, Phys. Rev. Lett. **114,** 257202 (2015).

[58] H. Kurebayashi, J. Sinova, D. Fang, A. C. Irvine, T. D. Skinner, J. Wunderlich, V. Novák, R. P. Campion, B. L. Gallagher, E. K. Vehstedt, L. P. Zârbo, K. Výborný, A. J. Ferguson, and T. Jungwirth, Nat. Nanotechnol. **9,** 211 (2014).

[59] H. Li, H. Gao, L. P. Zârbo, K. Výborný, X. Wang, I. Garate, F. Doğan, A. Čejchan, J. Sinova, T. Jungwirth, and A. Manchon, Phys. Rev. B **91,** 134402 (2015).

[60] J. L. Collins, A. Tadich, W. Wu, L. C. Gomes, J. N. B. Rodrigues, C. Liu, J. Hellerstedt, H. Ryu, S. Tang, S.-K. Mo, S. Adam, S. A. Yang, M. S. Fuhrer, and M. T. Edmonds, Nature (London) **564,** 390 (2018).